Role of CeO_2-ZrO_2 Support for Structural, Textural and Functional Properties of Ni-based Catalysts Active in Dry Reforming of Methane

Andrzej Adamski[1,*], *Piotr* Legutko[1], *Katarzyna* Dziadek[1], *Ksenia* Parkhomenko[2], *Cyril* Aymonier[3], *Vladislav A.* Sadykov[4] and *Anne-Cécile* Roger[2]

[1] Jagiellonian University, Faculty of Chemistry, Gronostajowa 2, 30-387 Krakow, Poland
[2] Université de Strasbourg, Institut de Chimie et Procédés pour l'Energy, l'Environnement et al Santé, UMR 7515 CNRS, 25 rue Becquerel, 67087 Strasbourg Cedex 2, France
[3] Université de Bordeaux 1, Institut de Chimie de la Matière Condensée de Bordeaux, ICMCB-CNRS and ENSCPB, 87 rue du Dr. Albert Schweizer, 33608 Pessac Cedex, France
[4] Boreskov Institute of Catalysis, Pr. Lavrentieva 5 and Novosibirsk State University, Pirogova 2, 630090 Novosibirsk, Russia

Abstract. Positive environmental and technological contexts make dry methane reforming (DMR) an extensively studied reaction. During this process two main greenhouse gases CH_4 and CO_2 can be simultaneously converted into syngas – a mixture of CO and H_2. Supported-nickel is one of the most frequently applied DMR catalysts. Their activity depends mainly on Ni concentration, kind of its precursor and a deposition method. As DMR is a demanding high-temperature reaction, it requires not only an active but first a very stable catalyst. Structural, textural and functional properties of such support remain thus of crucial efficiency. Main aim of this work was to elucidate how the synthesis of CeO_2-ZrO_2 support obtained by supercritical fluid method (*i.e.* at temperature of 400°C under a pressure of 25 MPa), can influence the properties of Ni-based DMR catalysts. The supports of various compositions (CeO_2 content from 100 to 0 %), subsequently calcined at 800°C for 6h in air have been analyzed. Nickel was deposited from nitrate(V) precursor via classical wet impregnation. The final catalysts have been characterized structurally (XRD, RS), texturally (BET, SEM) and functionally (UV/Vis-DR, XPS). Catalytic tests in dry methane reforming reaction have been performed to determine activity and stability of the synthesized samples.

1 Introduction

Nowadays ceria-zirconia binary oxides belong to relatively frequently used catalytic supports for both metals and metal oxides deposited on their surfaces as catalytically active phases. A characteristic feature of these two oxides is their excellent mixing, leading usually to a formation of the corresponding solid solutions ($Ce_xZr_{1-x}O_{2-y}$) in full

* Corresponding author: adamski@chemia.uj.edu.pl

concentration range [1, 2]. Redox properties exhibited by such materials, controlled by both CeO_2/ZrO_2 ratio and phase composition of $Ce_xZr_{1-x}O_2$ solid solutions [3, 4], are intimately related with quite easy exchange of oxygen between a CeO_2-ZrO_2 binary oxide structure and the gas phase, dependently on gaseous oxygen pressure. Thus CeO_2-ZrO_2 binary systems are generally considered as good oxygen buffers and their particular properties are crucial also for many catalytic applications [5, 6]. One of the prominent industrial applications of CeO_2-ZrO_2 is that in, so called, automobile three-way-catalyst (TWC), where the support extensively assists in a catalytic cycle together with a deposited active phase, constituted by noble metals such as Pt, Rh or Pd [7, 8]. Due to its high thermal stability, applications of CeO_2-ZrO_2 as supports for transition metals (mainly nickel, copper and cobalt [*e.g.* 9, 10, 11]) in a high-temperature dry methane reforming (DMR) has recently gained growing attention [12, 13].

The CeO_2-ZrO_2 solid solutions may exist in three different phases, depending on temperature, the molar ratio of both oxide components, preparation conditions and presence of additives. Thus, for CeO_2 contents lower than 10 %, a monoclinic ($P2_1/c$) phase, whereas for CeO_2 contents higher than 80 %, a cubic phase ($Fm\bar{3}m$) have been identified [2, 14]. In the intermediate concentration region, the occurrence of both stable (*t*) and metastable (*t'* and *t''*) tetragonal phases ($P4_2/nmc$) have been confirmed. The *t'* structure can be derived from the cubic phase by the cation diffussionless phase transition, whereas the *t''* phase characterized by the lattice parameter ratio $a/c = 1$, is an intermediate one between the tetragonal *t'* and the cubic phase [2]. Actually, the phase boundaries are rather vague due to a fact that for the metastable tetragonal forms, distortions from the fluorite-type structure are rather easy and highly sensitive to particles size.

A satisfactory performance of a final ceria-zirconia-supported DMR catalyst is strongly related to both thermal resistance and preservation of a high temperature homogeneity of the CeO_2-ZrO_2 support. It was reported by many authors that these binary oxides obtained via conventional methods from aqueous solutions of nitrate or chloride precursors of ZrO_2 tend to loose their homogeneity under reducing DMR reactional conditions undergoing a progressive segregation [12, 15]. This effect is directly linked with the characteristic speciation of Zr(IV) ions in the corresponding aqueous solutions of ZrO_2 precursor, where zirconium component occurs in a form of hydroxo-aqua $[Zr(OH)_2 \cdot 4H_2O]_4^{8+}$ complexes of tetrahedral coordination [16]. Such coordination can be partially stabilized also within the final CeO_2-ZrO_2 binary system, facilitating its high-temperature evolution leading to a structural instability and a stepwise segregation. Such negative effect can be partially eliminated when a dedicated preparation procedure favoring a loose of the coordinated water ligands from Zr(IV) coordination sphere is applied. Presented in this work, a continuous synthesis in supercritical medium may be a good example of such a tailored way of synthesis and design of the CeO_2-ZrO_2 system. Another reasonable option to avoid high-temperature segregation of $Ce_xZr_{1-x}O_2$ solid solution is to use such organometallic precursors of ZrO_2 as *e.g.* $Zr(OBu)_4$, $Zr(acac)_4$, complexes of Zr with citric acid and ethylene glycol [17, 18].

In this paper the preparation of CeO_2-ZrO_2 samples in supercritical conditions will be presented as an interesting alternative to obtain NiO_x/CeO_2-ZrO_2 samples exhibiting more satisfactory catalytic properties in comparison to those observed for samples of CeO_2-ZrO_2 supports synthesized via classical methods. The crucial role of CeO_2-ZrO_2 support for structural, textural and functional properties of Ni-based catalysts active in dry reforming of methane will thus be particularly stressed.

There are three fundamental features usually attributed to an efficient catalytic support: i) well-developed surface area to host catalytically active sites, ii) high thermal, mechanical and chemical resistance to prevent a catalyst from sintering, attrition, elutriation or any type of chemical corrosion and iii) occurrence of various functional groups responsible for

stabilization and sometimes also for activation of a catalytically active deposited phase. The role of our CeO_2-ZrO_2 binary supports obtained by continues synthesis in supercritical medium will thus be discussed in this paper regarding the essential features mentioned above in respect to both NiO deposition and catalytic activity of the supported NiO_x/CeO_2-ZrO_2 samples in the DMR. In the figures below the selected results for $NiO_x/Ce_{0.5}Zr_{0.5}O_2$ catalyst - the most active in DMR, are presented.

2 Experimental

2.1 Preparation of the NiO_x/CeO_2-ZrO_2 samples

A series of nanostructural CeO_2-ZrO_2 supports of various compositions (CeO_2 content from 100 to 0 %) has been prepared by a supercritical fluid technique starting from aqueous or water-ethanol solutions of ammonium cerium(IV) and zirconium(IV) nitrates (Sigma-Aldrich) as precursors. The solutions of such precursors have been contacted at the mixing point between two injection lines at temperature of 150 °C prior to enter them into a home-made continuous-flow reactor in which temperature was fixed at 400 °C and pressure at 25 MPa. Temperature and pressure have been selected to exceed the critical parameters of the water-ethanol mixture with a 29:71 molar ratio (T_c = 283.55 °C, p_c = 11.69 MPa, NIST Standard Reference Database). Processes of forced hydrolysis, nucleation and growth of the CeO_2-ZrO_2 nanoparticles occurred thus under supercritical conditions. The residence time inside the reactor was equal to fifteen seconds. At the exit of the reactor the products were transferred to a cold zone to quench the further particle growth. The final nanoparticles were collected, centrifuged and dried at ambient conditions. The binary samples of Ce:Zr ratios corresponding to 0.25:0.75, 0.50:0:50 and 0.75:0.25 have been synthesized together with the undoped CeO_2 and ZrO_2 single oxides. In the next step all fresh samples were calcined at 800 °C for 6 h in air with a heating rate of 4 °C /min.

10 wt.% of nickel was deposited on all the calcined supports using classical wet impregnation using appropriate amount of $Ni(NO_3)_2{\cdot}6H_2O$ aqueous solution as precursor. Each time a portion of 0.15-0.20 g of a support was impregnated. The final NiO_x/CeO_2-ZrO_2 preparations were stirred for 1 h, dried at 100 °C for 8 h and subsequently calcined at 800 °C for 6 h in air with the heating rate of 4 °C min^{-1}.

2.2 Characterization of the NiO_x/CeO_2-ZrO_2 samples

X-ray diffraction patterns (XRD) were recorded by means of a *Bruker* D8 Advance diffractometer with a LynxEye detector and Ni filtered Cu K_α radiation (1.5418 Å) over a 2θ range of 10–90° and a position-sensitive detector using a step size of 0.012° and a step time of 0.5 s.

The Raman spectra were recorded at room temperature in the range of 100 to 3500 cm^{-1} with 1 cm^{-1} resolution. The Raman spectrometer used was a DXR dispersive microscope with a 532 nm wavelength excitation laser, operating at 8 mW output power.

Specific surface areas measurements were carried out by nitrogen adsorption–desorption method at -196°C using the Brunauer–Emmet–Teller (BET) technique on a *Micromeritics* ASAP 2420 apparatus. The analyzed samples were previously outgassed at 250°C for 3 h to remove the adsorbed moisture.

Scanning electron microscopy (SEM) micrographs were recorded on a JEOL FEG 6700F microscope working at 9 kV accelerating voltage.

The diffuse reflectance ultraviolet/visible (UV/Vis-DR) spectra of the investigated samples were recorded using a *Perkin-Elmer* Lambda 650 UV/Vis spectrophotometer with Praying

Mantis (*Harrick*). The measurements were performed in the range of 200–900 nm with a resolution of 1 nm. The spectra were recorded under ambient conditions and the data transformed according to the Kubelka-Munk equation. Deconvolution of spectra was carried out using *PeakFit4* software.

The X-ray photoelectron spectroscopy (XPS) analyses were carried out in a *PHI* VersaProbeII Scanning XPS system using monochromatic Al K_α (1486.6 eV) X-rays focused to a 100 μm spot and scanned over the sample area of 400 μm x 400 μm. The photoelectron take-off angle was 45° and the pass energy in the analyzer was set to 23.50 eV to obtain high energy resolution spectra for the C 1s, O 1s, Zr 3d, Ce 3d and Ni 2p regions. A dual beam charge compensation with 7 eV Ar^+ ions and 1 eV electrons were used to maintain a constant sample surface potential regardless of the sample conductivity. All XPS spectra were charge referenced to the unfunctionalized, saturated carbon C1s peak at 284.8 eV. The operating pressure in the analytical chamber was below $4 \cdot 10^{-9}$ mbar. Deconvolution of spectra was carried out using *PHI* MultiPak software (v.9.7.0.1). Spectrum background was subtracted using the Shirley method.

2.3 Catalytic tests

A mixture of gases with a total flow 70 ml/min (N_2 = 5 ml/min, Ar = 45 ml/min, CH_4 = 10 ml/min, CO_2 = 10 ml/min) was fed into a quartz reactor. Total flow was adjusted with five flowmeters and a mass flow controller (*Brooks Industry*). Quartz reactor was placed in the oven, where temperature was controlled with temperature programmer. 0.01 g of catalyst was mixed with 0.03 g of silicon carbide. The catalyst bed was supported on quartz wool and quartz chips. Reactants passed through fluid trap and analyzed by gas chromatograph (*Agilent Technologies* 6890N Network GC System). Firstly, a catalyst was reduced at 450°C with pure H_2 flow (10 ml/min) for 120 min. After reaching 500°C H_2 flow was switch off and other gaseous reactants were turn on. Gas chromatographic measurements was performed from RT every 50°C up to 800°C and at one back point (650°C).

3 Results and discussion

3.1 Textural properties

As it can be seen in Fig. 1. below, in the case of a representative $NiO_x/Ce_{0.5}Zr_{0.5}O_2$ sample, the continues synthesis under supercritical conditions leads to a satisfactory surface development of mainly mesoporous character, confirmed by a characteristic shape of the corresponding adsorption-desorption hysteresis loop (type IV, according to IUPAC classification [19]). The mesopores are most probably of cylindrical shapes for all investigated fresh samples and quite uniform in diameters, ranging from *ca.* 4 to 10 nm.

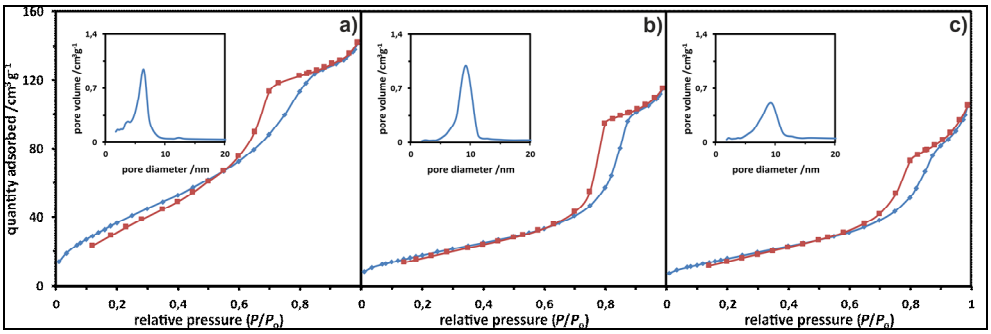

Fig. 1. The N_2 adsorption/desorption isotherms and the corresponding pore distribution for fresh (a), calcined (b) and impregnated with nickel nitrate (c) $Ce_{0.5}Zr_{0.5}O_2$ support.

Unsurprisingly, calcination at 800°C resulted in a visible shift in pore diameters towards slightly higher values. The observed shifts corresponded to sample compositions. Deposition of NiO did not result in any remarkable changes of average textural parameters, however a slightly broader pore distributions can be confirmed for NiO_x/CeO_2-ZrO_2 samples, comparing to those characteristic of CeO_2-ZrO_2 supports. The determined specific surface areas (SSA) remained quite high for the fresh supports, reaching 117-150 m^2/g and dropping down to 20–70 m^2/g after calcination. Introduction of NiO onto the CeO_2-ZrO_2 surfaces, resulted in SSA stabilization in the range 31–64 m^2/g.

A characteristic flowers- or flakes-like morphologies were visible in the SEM images recorded for the fresh samples of the investigated CeO_2-ZrO_2 supports (not shown here). Thermal treatment of these samples at 800°C was responsible mainly for a progressive agglomeration of nanograins and for their more close packing. Deposition of NiO did not change neither granulation nor spatial arrangement of the studied preparations in any remarkable extent.

It can be stated that the continues synthesis under supercritical conditions, applied in this work, permits to obtain the CeO_2-ZrO_2 supports of quite promising textural properties, suitable for NiO stabilization and subsequent use of the final catalysts at high temperature DMR reaction.

3.2 Phase and structural compositions

Phase and structural compositions of a support are absolutely crucial for stability of a final catalyst. These properties cannot also be neglected at considering the nature of interaction between catalytic support and a deposited active phase. Hence, structural features of a support surface remain of vital importance for catalytic performance of the studied system.

XRD patterns collected for all investigated non-calcined CeO_2-ZrO_2 samples synthesized in supercritical conditions resemble that recorded for $Ce_{0.5}Zr_{0.5}O_2$ (shown in Fig. 2Aa) and match quite well to that registered for pure ceria of regular structure (ICDD: 01-081-0792). The reflections characteristic of CeO_2 were identified at 2θ positions of *ca.* 28.5, 33.5, 48 and 57°, originating from (111), (200), (220) and (311) crystallographic planes, respectively. The presence of zirconia in binary samples resulted in visible shifts of the corresponding reflections, previously ascribed to ceria, to higher values of 2Θ angles. This effect can be explained by incorporation of Zr^{4+} ions into the cationic sublattice of CeO_2, leading to a formation of the corresponding $Ce_xZr_{1-x}O_2$ solid solutions. The formation of such phases was suggested for CeO_2-ZrO_2 binary oxides also by many authors [2, 4, 12, 13, 20]. Basically, the investigated supports were single phases of high homogeneity. Only in the case of $Ce_{0.25}Zr_{0.75}O_2$ sample an admixture of the regular CeO_2

phase was suggested by XRD. It is worthy to note that even before calcination, any presence of amorphous phases was observed. This means that supercritical conditions can be specifically recommended for synthesis of catalytic support, permitting to obtain well crystalline preparations immediately. Moreover, as it can be inferred from the recorded XRD patterns, after thermal treatment of our support samples at 800°C, their initial structures were preserved. The slight sharpening of the XRD maxima (visible in Fig. 2Ab) is a simple consequence of crystallites growth due to thermally-induced grain sintering. In the case of NiO_x/CeO_2-ZrO_2 samples, the weak Bragg reflections, characteristic of NiO nanocrystallites, appeared in the XRD patterns (Fig. 2Ac). This means that the support surface did not undergo wetting by the deposited oxide. Rather weak interaction between support and deposited phase are thus suggested.

The average diameters of the fresh CeO_2-ZrO_2 binary oxide grains, determined by Scherrer method, were around 6.3-6.5 nm, *i.e.* slightly lower than that determined for CeO_2, which was equal to 7.5 nm. It can also be confirmed that catalyst grains grow with calcination, reaching the diameters around 8.5-11.3 nm. The reported data clearly suggest that our synthesis of CeO_2-ZrO_2 in superciritical medium permits to obtain the preparations of distinctly smaller crystallites of much more uniform phase compositions in comparison to those synthesized via alternative methods [13, 21, 22]. Simultaneously, in the case of all investigated catalysts, NiO crystallites were determined to remain larger (12.3-14.3 nm) in comparison to the crystallites of the calcined binary supports. This is another evidence for rather poor dispersion of the NiO deposited phase and quite weak adhesive interaction of the deposited phase with the used CeO_2-ZrO_2 supports, independently on their compositions.

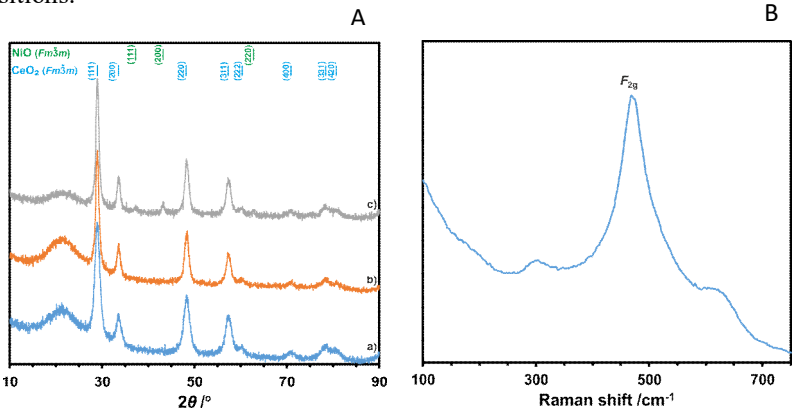

Fig. 2. A. Diffraction patterns of the investigated $Ce_{0.5}Zr_{0.5}O_2$ support: before calcination (a), after calcination at 800°C (b), after impregnation with nickel nitrate (c); B. Raman spectrum of the as prepared $Ce_{0.5}Zr_{0.5}O_2$ support.

Structural information obtained from the analysis of Raman results remained in accordance with those inferred from XRD patterns. As it can be seen in the case of a representative RS spectrum, recorded for the fresh $Ce_{0.5}Zr_{0.5}O_2$ sample and shown in Fig. 2B, an intense peak peak can be observed at 470 cm^{-1} and accompanied by two weaker peaks at *ca.* 310 and 620 cm^{-1}. The maximum predominating the spectrum can be attributed to a symmetrical F_{2g} Raman active mode typical of the fluorite-like regular structure of CeO_2 [13]. The peak at lower Raman shift can be ascribed to the vibrations associated with oxygen anions located at the positions slightly shifted from those characteristic of the ideal fluorite lattice due to the introduction of Zr^{4+} into the cationic sublattice of CeO_2 [22,23], whereas an appearance of the peak at 620 cm^{-1} was most probably associated with the vacancies created in anionic sublattice [22,23].

Surface structure of the investigated CeO_2-ZrO_2 supports and NiO_x/CeO_2-ZrO_2 catalysts was studied by XPS. Representative results obtained for $Ce_{0.5}Zr_{0.5}O_2$ sample (fresh, calcined and impregnated with the NiO precursor) are presented in Fig 3a-c below. Spectral window characteristic of Ce3d reflected rather complex structure due to both spin-orbital splitting and the coexistence of both Ce(III) and Ce(IV) states [13]. As it can be assumed basing on the spectra, main oxidation state of cerium was Ce^{4+} and only the traces of Ce^{3+} contributed to the recorded spectra. In turn, an inspection of the region characteristic of Zr 3d of the XPS spectra can be interpreted as originating from both Zr $3d_{5/2}$ and Zr $3d_{3/2}$ states. The positions of the characteristic doublet clearly suggested Zr^{4+} as the more abundant.

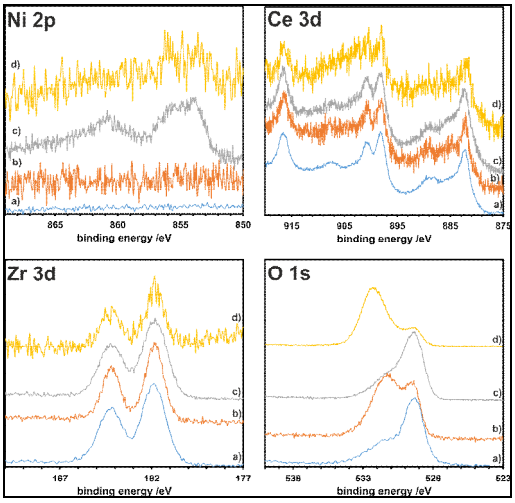

Fig. 3. Ni 2p, Ce 3d, Zr 3d and O 1s windows of the XPS spectra recorded for $Ce_{0.5}Zr_{0.5}O_2$ supports: fresh (a), calcined (b), impregnated with nickel nitrate (c) and after DMR reaction (d).

Contrary to the status of both previous elements in the investigated samples, giving rise to the discussed XPS spectra and practically unchanged by thermal treatment or NiO deposition, the peaks characteristic of O 1s at *ca.* 529-530 eV and at *ca.* 531-533 eV, attributed to both lattice oxygen and to so called defect (usually meant as chemisorbed or hydroxyl/carbonate-related) oxygen, respectively [24], clearly mirrored structural evolution of the investigated system. The relative amount of lattice oxygen was higher for non-calcined samples and increases after NiO deposition. It was quite interesting that for the samples analyzed after DMR test, the trend related to the intensity ratio of two types of the observed oxygen species, contributing to O 1s window and discussed above, was opposite to that described for samples before catalytic test (as it can be seen in Fig. 3d) – defect oxygen predominated the XPS spectra. This effect can be related with a strong involvement of mobile oxygen in the oxidation of carbon deposits occurring on the surface of the investigated samples.

Obviously, the Ni^{2+} species contributed only to the XPS spectra recorded for NiO_x/CeO_2-ZrO_2 samples. As it can be concluded from the deconvoluted XPS spectra, two types of nickel(II) centers should be taken into account – oxide and hydroxide, giving rise to the window between 852 and 863 eV.

Structural analysis presented above confirmed quite homogeneous monophase character of the obtained CeO_2-ZrO_2 samples and their relatively weak dispersing effect towards the deposited NiO. Simultaneously, the deposited phase was stabilized in two different forms.

3.3 Main functional features and catalytic behavior

As the reactivity of the investigated samples in DMR reaction is strongly dependent on their electronic properties, UV/Vis-DR spectra recorded for both calcined CeO_2-ZrO_2 supports and impregnated with nickel nitrate, provided some insight into essencial functional features of the studied system. The corresponding spectra recorded for $Ce_{0.5}Zr_{0.5}O_2$ are shown in Fig. 4A below as an example. Both ligand-to-metal $Ce^{3+} \leftarrow O^{2-}$ and $Ce^{4+} \leftarrow O^{2-}$ charge transfer transitions at *ca.* 230 nm and 275 nm as well as an interband transitions (at ca. 340 nm) were observed in the UV/Vis-DR spectra recorded for all investigated samples. This result remains in agreement with interpretation of the XPS spectra suggesting the coexistence of both cerium oxidation states. For the samples of higher amount of zirconium (50% and more) also a corresponding ligand-to-metal $Zr^{4+} \leftarrow O^{2-}$ charge transfer transitions were observed, giving rise to the band at *ca.* 250 nm. Except of those related to NiO, the electronic transitions characteristic of the studied impregnated NiO_x/CeO_2-ZrO_2 samples contributing to the UV/Vis-DR spectra were in principle the same as it was observed for the corresponding CeO_2-ZrO_2 binary supports. The transitions attributed to NiO can be observed in all recorded spectra: d-d transitions between adjacent Ni^{2+} centers at ca. 400 nm [26], 3d-3d interatomic transitions at *ca.* 300 nm [26], ligand-to-metal $Ni^{2+} \leftarrow O^{2-}$ charge transfer transitions at *ca.* 270 nm [27], and ${}^3A_{2g} \rightarrow {}^1T_{2g}(P)$ transitions of Ni^{2+} centers in octahedral symmetry at *ca.* 725 nm [26, 27]. The diffused band shifted to higher wavelengths, ascribed to the transitions within the bulk of NiO, was more intense for Ni/CeO_2 than for other analyzed samples.

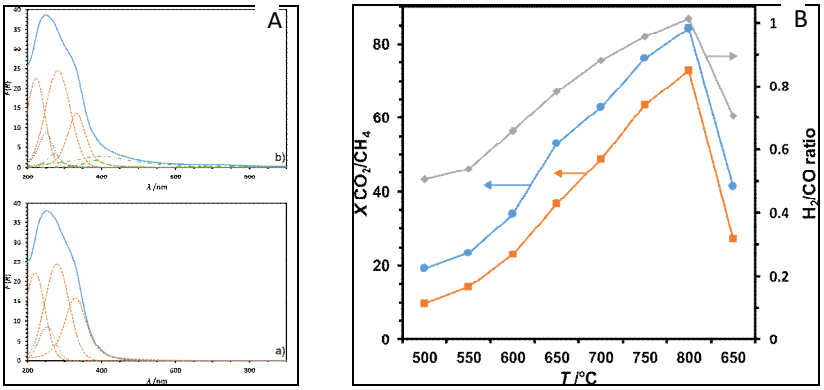

Fig. 4. A. UV/Vis-DR spectra of the $Ce_{0.5}Zr_{0.5}O_2$ support calcined at (a) and impregnated with nickel nitrate (b). Deconvoluted spectra: orange dashed line – cerium-related transitions, grey dotted line – zirconium-related transitions, green dots and lines – nickel-related transitions; B. Catalytic activity of the $Ni/Ce_{0.5}Zr_{0.5}O_2$ sample in DMR: conversion of carbon dioxide (squares), conversion of methane (squares), and hydrogen to carbon monoxide ratio (diamonds) as a function of reaction temperature.

It can be stated basing on the results of catalytic tests carried out for the studied NiO_x/CeO_2-ZrO_2 samples, that all of them are active in DMR, independently on the support composition. The $NiO_x/Ce_{0.5}Zr_{0.5}O_2$ sample may be considered as the most active in the investigated series (*cf.* Fig. 4B), even despite the fact that regarding their catalytic parameters, the samples behaved quite similarly. The investigated NiO_x/CeO_2-ZrO_2 catalysts showed *ca.* 70% and 80% conversions of CH_4 and CO_2, respectively, and the observed activities were quite satisfactory, even if the decrement of activity of the back point at 650°C can be significant for partial deactivation of our catalysts. No by-products have been detected. Catalytic tests confirmed also relatively high thermal stability of the investigated samples and a favorable H_2 : CO ratio, close to 1: 1.

The catalytic results reported above confirmed the promising activity of the investigated series of NiO_x/CeO_2-ZrO_2 samples in dry reforming of methane, permitting to obtain the H_2 : CO products ratio, which is the most suitable for synthetic fuel production. Moreover, the CeO_2-ZrO_2 supports obtained via continuous synthesis in supercritical medium substantially enhanced the thermal stability of the studied catalysts, making them applicable in such demanding reactions as DMR. Catalytic activity can be ascribed to nickel sites initially stabilized within oxide and hydroxide surface complexes.

4 Conclusions

In this study, a series of the supported Ni-catalysts based on binary ceria-zirconia carriers, synthesized by continuous method in supercritical medium, was investigated by several techniques. It was confirmed within the current work, that the presence of $Ce_xZr_{1-x}O_2$ solid solutions was characteristic of the studied binary supports. The CeO_2-ZrO_2 oxide samples exhibited favorable structural and textural properties such as relatively high homogeneity, good thermal stability, satisfactory surface area and porosity. Contrary to these, interactions between nickel-containing deposited phase and the CeO_2-ZrO_2 supports were not entirely suitable prior to the DMR reaction (favoring the progressive reduction of Ni centers), because of the relatively poor dispersion of Ni-entities, occurring initially in both oxide and hydroxide forms. Despite this fact, the catalytic activity of the investigated samples in dry reforming of methane reached *ca.* 80% of conversion at temperature of 800°C for all investigated samples except of that for NiO_x/CeO_2. A sample containing 10 wt. % of Ni supported on $Ce_{0.5}Zr_{0.5}O_2$ can be considered as the most active, even if the differences in the catalytic behavior between this sample and the other ones supported on binary supports were not very pronounced. In conclusion it can be thus stressed that the NiO_x/ceria-zirconia catalytic system exhibited both promising catalytic performance and stability in the DMR tests. It is also worthy to note, that the design of nanomaterials for dedicated catalytic purposes using a continuous supercritical preparation technique is not only possible by also it permits to obtain the DMR catalysts of an increased resistance to deactivation. It was revealed within the current studies that both structural and textural properties of our supports were crucial for the high-temperature stability of the investigated NiO_x/CeO_2-ZrO_2 catalysts.

This work has been carried out in the framework of the *NiCe* ERANet RusPlus S & T project. The Polish authors thank for the financial support from National Centre for Research and Development (Agreement No.: 5/RUSPLUS – S&T/2016).

References

1. D. Hari Prasad, J.-H. Lee, H.-W. Lee, B.-K. Kim, J.-S. Park, Ceram. Proc. Res. **10**, 6 (2009)
2. A. Trovarelli (Ed.), *Catalysis by Ceria and Related Materials* (Imperial College Press, London, 2002)
3. G.Vlaic, R. Di Monte, P. Fornasiero, E. Fonda, J. Kašpar, M. Graziani, Stud. Surf. Sci. Catal. **116**, 185 (1998)
4. R. Di Monte, J.Kašpar, J. Mater. Chem. **15**, 633 (2005)
5. T. Montini, M. Melchionna, M. Monai, P. Fornasiero, Chem. Rev., **116**, 5987 (2016)
6. D. Devaiah, L.H. Reddy, S.-E. Park, B.M. Reddy, Catal. Rev. Sci. Eng., **60**, 177 (2018)
7. J. Kašpar, P. Fornasiero, M. Graziani, Catal. Today, Catal. **119**, 114 (2007)

8. J. Wang, H. Chen, Zh. Hu, M. Yao, Y. Li, Catal. Rev. Sci. Eng., **57**, 79 (2015)
9. Th.A. Maia, E.M. Assaf, RCS Advances, **4**, 31142 (2014)
10. D.-W. Jeong, H.-S. Na, J.-O. Shim, W.-J. Jang, H.-S. Roh, Catal. Sci. Technol., **5** 3706 (2015)
11. S.S.-Y. Lin, H. Daimon, S.Y. Ha, Appl. Catal. A, **366**, 252 (2009)
12. A. Kambolis, H. Matralis, A. Trovarelli, Ch. Papadopoulou, Appl. Catal. A, **377**, 16 (2010)
13. V.A. Sadykov, M.N. Simonov, N.V. Mezentseva, S.N. Pavlova, Y.E. Fedorova, A.S. Bobin, Y.N. Bespalko, A.V. Ishchenko, T.A. Krieger, T.S. Glazneva, T.V. Larina, S.V. Cherepanova, V.V. Kaichev, A.A. Saraev, Y.A. Chesalov, A.N. Shmakov, A.-C. Roger, A. Adamski, Open Chem. (De Gruyter), **14**, 363 (2016)
14. A. Adamski, E. Tabor, B. Gil, Z. Sojka, Catal. Today, **119**, 114 (2007)
15. R. Grau-Crespo, N.H. De Leeuw, S. Hamad, U.V. Waghmare, Proc. R. Soc. A, **467**, 1925 (2011)
16. P. Jakubus, A. Adamski, M. Kurzawa, Z. Sojka, J. Thermal. Anal. Calorim., **72** 299 (2003)
17. M.Yu. Smirnova, A.S. Bobin, S.N. Pavlova, A.V. Ishchenko, A.V. Selivanova, V.V. Kaichev, S.V. Cherepanova, T.A. Krieger, M.V. Arapova, A.-C. Roger, A. Adamski, V.A. Sadykov, Open Chem. (De Gruyter), **15**, 412 (2017)
18. A.N. Shmakov, S.V. Cherepanova, D.A. Zyuzin, Y.E. Fedorova, I.A. Bobrikov, A.-C. Roger, A. Adamski, V.A. Sadykov, Open Chem. (De Gruyter), **15**, 438 (2017)
19. K. Periyasamy, V.T. Aswathy, RSC Adv. **5**, 3619 (2015)
20. A. Horváth, G. Stefler, O. Geszti, A. Kienneman, A. Pietraszek, L. Guczi, Catal. Today, **169,** 102 (2011)
21. A. Wolfbeisser, O. Sophiphun, J. Bernardi, J. Wittayakun, K. Föttinger, G. Rupprechter, Catal. Today, **277**, 234 (2016)
22. J.A. Montoya, E. Romero-Pascual, C. Gimon, P. Del Angel, A.Monzónet, Catal. Today, **63**, 71 (2000)
23. B.M. Reddy, P. Lakshmanan, A. Khan, J. Phys. Chem. B, **109**, 13545 (2005)
24. L. Liu, Z. Yao, B. Liu, L. Dong, J. Catal., **275**, 45 (2010)
25. A.E. Nelson, K.H. Schulz, Appl. Surf. Sci., **210**, 206 (2003)
26. T. Isobe, S.Y. Park, R.A. Weeks, R.A. Zuhr, J. Non-Cryst. Solids, **189**, 173 (1995)
27. S. Damyanova, B. Pawelec, K. Arishtirova, J.L.G. Fierro, Int. J. Hydrog. Energy, **37**, 15966 (2012)